Engineering Structures 176 (2018) 734–745

Contents lists available at ScienceDirect

Engineering Structures

journal homepage: www.elsevier.com/locate/engstruct

Simplified design of elastoplastic structures with metallic yielding dampers based on the concept of uniform damping ratio

Ruifu Zhang[a], Chao Wang[a], Chao Pan[b,*], Hua Shen[a], Qingzi Ge[c], Luqi Zhang[a]

[a] Research Institute of Structural Engineering and Disaster Reduction, Tongji University, Shanghai 200092, China
[b] College of Civil Engineering, Yantai University, Yantai 264005, China
[c] Sichuan Institute of Building Research, Chengdu 610081, China

ARTICLE INFO

Keywords:
Uniform damping ratio concept
Seismic energy dissipation
Metallic yielding damper
Elastoplastic structure
Demand-oriented design

ABSTRACT

This study proposes a novel design concept, referred to as the uniform damping ratio (UDR) concept, to improve the seismic energy dissipation efficiency of damped structures with metallic yielding dampers (MYDs) by maximizing the use of the capability of each damper. Furthermore, this new concept can simplify the design procedure of structures with MYDs. The UDR concept implies that all installed MYDs have the same equivalent damping ratio under dynamic excitations, which enables each MYD to be fully utilized. The UDR concept can simplify the estimation process of the additional equivalent damping ratio of a damped structure and decouple the stiffness and damping effects caused by MYDs, which can be designed separately. A performance demand-oriented design procedure is presented based on the UDR concept considering the nonlinear properties of an original structure and MYDs under an intense earthquake. The design procedure involves the following three steps: (1) determine seismic performance demand and obtain the elastic and elastoplastic properties of the original structure using pushover analysis; (2) determine key design parameters based on the formulae derived under the UDR concept; (3) verify seismic performance via nonlinear dynamic analyses. In addition, a few empirical suggestions are provided for determining the key design parameters more efficiently. A nine-story steel frame structure with MYDs is used to exemplify the UDR-based design procedure. The seismic performance demand of the structure with designed MYDs is achieved, and the energy dissipation capacity of all installed MYDs is sufficiently utilized. The proposed UDR concept is found to be effective, and the procedure based on this concept is efficient and simple.

1. Introduction

Numerous studies and engineering applications have demonstrated that seismic energy dissipation technology [1,2] is a feasible and efficient approach to mitigate seismic damage to structures and improve their seismic performance [3–8]. The dissipation mechanism of a structure with energy dissipation devices involves absorbing and dissipating seismic input energy via dampers installed at appropriate locations in the structure [9,10]. Therefore, the dynamic response of the structure is suppressed, protecting it from unrecoverable damage. The energy dissipation concept has been employed in the seismic design codes in several countries because of its positive effect on improving the seismic performance of structures [11–13].

Various types of energy dissipation devices are currently employed for damped structures. In particular, the metallic yielding damper (MYD) pioneered by Kelly et al. [14] is one of the popular devices for numerous researchers and engineers because of its simple construction, lower cost, stable performance, and simple mechanical model [15–20]. Numerous analytical and experimental investigations have been conducted on techniques to increase structural dissipation capacity via MYDs [21–25]. Popular devices include shear yielding dampers [26,27], bending yielding dampers [28,29], and axial yielding dampers [30–32]. The hysteretic behavior of MYDs can be described using bilinear hysteretic models [33] or smooth hysteretic models (Ramberg–Osgood model [34] and Bouc–Wen model [35,36]). The characteristic parameters include initial stiffness k_{d0}, yielding force F_{dy}, and yielding displacement u_{dy}, which should be appropriately determined in the design stage [37–39]. Appropriate design theories and methods are necessary to promote the engineering application of MYDs for energy dissipation. The current design codes [11–13] for damped structures have covered numerous design principles, including discussions on the analytical models of dampers, performance demand [20,40], and

* Corresponding author.
E-mail address: panchao@ytu.edu.cn (C. Pan).

https://doi.org/10.1016/j.engstruct.2018.09.009
Received 17 February 2018; Received in revised form 20 August 2018; Accepted 8 September 2018
Available online 24 September 2018
0141-0296/

analytical methods for the seismic response of structures. Moreover, a large number of researchers have proposed different design methods based on different design principles [41–45]. For example, the Japan Society of Seismic Isolation recommends using the damping performance curve of a single-degree-of-freedom (SDOF) system to determine the design parameters of dampers [46]. Lee and Kim [47] proposed a design procedure based on the capacity spectrum method for the seismic retrofit of building structures with MYDs. Benavent-Climent and Mota-Páez [48] proposed an energy-based procedure to determine the strength, stiffness, and energy dissipation capacity of dampers, wherein the main structure largely remained in the elastic stage. However, the main structure can exhibit plastic behavior under moderate and severe earthquakes; hence, considering the plastic behavior of the main structure in practical design is reasonable. This was typically neglected in the abovementioned methods. Accordingly, an improved performance-based design method considering the inelastic behavior of the main structure has been proposed to resolve this issue [49–53]. Lin et al. [51] proposed a direct displacement-based design method and derived design equations to determine the equivalent linearized parameters of various dampers. However, the damping ratio of the dampers was determined based on experience. Shen et al. [54] proposed a design method for a structure with MYDs based on the elastoplastic response reduction curve. As the accumulated energy dissipation under seismic events is another important cause of structural damage, energy-based design methods have been proposed for structures with MYDs [55–57]. Choi and Kim [56] proposed an energy-based seismic design method for buckling-restrained braced frames using hysteretic energy spectra and cumulative ductility strength spectra. This method has an explicit physical meaning and helps effectively control the seismic performance of structures. However, further investigations are required for its practical applications because of the lack of widely applicable hysteretic energy spectra and cumulative ductility strength spectra.

With the development of high-performance scientific computation, a few researchers have proposed numerical optimal design methods for passive energy dissipation systems to simultaneously increase the energy dissipation efficiency of dampers and reduce cost [58,59]. These methods aim to optimize the locations and specifications of dampers to obtain the best performance at lower cost. The parametric design of dampers in these methods requires numerous dynamic time history analyses, which are time consuming because of the elastoplasticity or nonlinearity of structures, particularly for complex structures and high-rise structures. Moreover, responses vary considerably under different seismic excitations, and no widely recognized quantitative principle is followed for the selection of seismic waves in current design codes or regulations. Hence, the reliability and feasibility of these parametric design approaches remain topics for further investigation.

Even though the inelastic behavior of the main structure was considered in the abovementioned design methods, they are still considerably complex to implement because in most existing methods, stiffness and damping parameters are coupled and they must be considered together when designing structures with MYDs. This makes the design procedure more complex. Moreover, not all MYDs can be fully utilized in these methods.

This study presents a succinct design concept, referred to as the uniform damping ratio (UDR) concept, to effectively simplify the design procedure and fully utilize each damper. The formula for estimating the equivalent additional damping ratio can be simplified based on the UDR concept. Furthermore, the stiffness and damping effects caused by MYDs can be decoupled. Thus, the design procedure can be simplified. An SDOF system equivalent to the original structure is employed to estimate the seismic response of a damped structure in the parametric design of dampers and to reduce computational effort. The well-known pushover analysis is incorporated in the UDR method to consider the elastoplastic behavior of the original structure. Moreover, the parametric determination process is performance demand-oriented in achieving a rational and practical design. The proposed method is verified using a nine-story structure. Structural seismic performance is validated through nonlinear time history analysis. The results show that the simplified method is effective with acceptable precision.

2. Design philosophy

2.1. Design concept

From a conceptual perspective, a fairly ideal seismic energy dissipation effect can be obtained if each damper installed in a structure is fully utilized. The degree of utilization of an MYD can be reflected by its equivalent viscous damping ratio. Consequently, a novel design concept, referred to as the UDR concept, is used to effectively utilize each damper for seismic energy dissipation. The UDR concept implies that the equivalent damping ratios of all installed dampers are expected to be the same (i.e., a constant) under a certain dynamic excitation. By fully utilizing dampers, the UDR concept can result in less or smaller dampers under a specified performance demand, which can be considered as implicit optimization effectiveness even if there are no mathematical optimization approaches involved.

In addition to the damping property, MYDs can significantly influence the stiffness of a damped structure. Notably, high supplemental stiffness helps effectively control the displacement of a structure. However, the smaller displacement of MYDs may restrict their energy dissipation function. Moreover, high supplemental stiffness may cause larger inertial force under seismic excitation, resulting in increase in internal forces such as the story shear forces and axial forces of columns and the additional nodal forces caused by braces within a structure. Therefore, as two key design components, stiffness and damping should be balanced for an ideal design of structures with MYDs.

Table 1 presents the notations used in this study.

2.2. Key parameters for design

The equivalent viscous damping ratio of an MYD, $\xi_{dd,i}$, can be calculated as follows by matching the energy dissipated by plasticity and the energy dissipated by viscous damping [60]:

$$\xi_{dd,i} = \frac{W_{d,i}}{4\pi W_{sd,i}} \tag{1}$$

where $W_{d,i}$ is the dissipated energy of the damper during one vibration cycle, $W_{sd,i}$ is the elastic strain energy of the damper, and subscript "i" denotes the index of dampers.

The damper-supplied additional equivalent viscous damping ratio, ζ_{da}, can be evaluated using the strain energy method, as follows [60]:

$$\zeta_{da} = \frac{\sum W_{d,i}}{4\pi W_s} = \frac{\sum W_{sd,i}}{W_{s0} + \sum W_{sd,i}} \cdot \frac{\sum W_{d,i}}{4\pi \sum W_{sd,i}} \tag{2}$$

where $\sum W_{d,i}$ is the summation of the hysteretic energy dissipated by all dampers in one vibration cycle. $W_s = W_{s0} + \sum W_{sd,i}$ is the elastic strain energy of the damped structure (summation of the strain energies of the structure and dampers).

Eq. (2) shows that ζ_{da} is a product of two fractions. The first fraction is defined as the generalized additional stiffness ratio and denoted as κ. It is the ratio of the total strain energy of dampers to the total strain energy of the system.

$$\kappa = \frac{\sum W_{sd,i}}{W_{s0} + \sum W_{sd,i}} = \frac{\sum W_{sd,i}}{W_s} \tag{3}$$

The second fraction in Eq. (2) can be simplified as follows if the damping ratio of each damper is the same (i.e., $\xi_{dd,i} = \xi$):

$$\frac{\sum W_{d,i}}{4\pi \sum W_{sd,i}} = \frac{\sum 4\pi\xi_{dd,i} W_{sd,i}}{4\pi \sum W_{sd,i}} = \frac{4\pi\xi \sum W_{sd,i}}{4\pi \sum W_{sd,i}} = \xi \tag{4}$$

Eq. (2) can now be rewritten as follows:

Table 1
Notations.

Notation	Definition
$W_{d,i}$	Dissipated energy of an MYD for one hysteretic cycle
$W_{sd,i}$	Elastic strain energy of an MYD for one hysteretic cycle
W_s	Elastic strain energy of the damped structure
W_{s0}	Elastic strain energy of the original structure
W_{ps}	Nonlinear plastic hysteresis energy of the original structure
κ	Generalized additional stiffness ratio
$\xi_{dd,i}$	Equivalent viscous damping ratio of an MYD
ξ	Uniform damping ratio of an MYD
ζ_{da}	Damper-supplied additional equivalent viscous damping ratio
ζ_{s0}	Nonlinear plastic hysteretic damping ratio of the original structure
ζ_s	Nonlinear plastic hysteretic damping ratio of the damped structure
ζ_{eq}	Equivalent damping ratio of the damped structure system
ζ_0	Inherent damping ratio of the original structure
m_n	Story mass
M_{eq}	Equivalent mass of the structure
$K_{eq,s}$	Equivalent stiffness of the original structure
$T_{eq,s}$	Equivalent period of the original structure
K_{eq}	Equivalent stiffness of the damped structure
T_{eq}	Equivalent period of the damped structure
k_n	Story stiffness
$k_{d0,n}$	Initial stiffness of MYDs on the nth story
$k_{d,n}$	Effective stiffness of MYDs on the nth story
k_{de}	Elastic stiffness of MYDs
$\{\widetilde{k}_n\}$	Normalized story stiffness vector of the original structure
$\{\widetilde{k}_{d,n}\}$	Normalized effective stiffness vector of MYDs
$k_{d0,nj}$	Initial stiffness of the jth MYD on the nth story
α	Post-to-pre-yielding stiffness ratio of MYDs
F_d	Damping force of MYDs
$F_{dy,n}$	Yielding force of MYDs on the nth story
$F_{dy,nj}$	Yielding force of the jth MYD on the nth story
u_n	Story displacement
u_{top}	Top displacement
Δu_n	Interstory displacement
$\Delta\overline{u}_n$	Average interstory displacement of the nth story
$\Delta u_{n,j}$	Interstory displacement at the location of the jth damper
ϕ_n	Normalized story displacement
δ_n	Normalized interstory displacement
$u_{d,n}$	Displacement of MYDs on the nth story
$u_{dy,n}$	Yielding displacement of MYDs on the nth story
μ	Ductility factor of MYDs
μ_u	Ultimate ductility factor of MYDs
μ_{Lu}	Ductility factor of MYDs under the highest fortification level earthquake
μ_{Li}	Ductility factor of MYDs corresponding to the ith performance level
V_{base}	Base shear force
S_d	Spectrum displacement
$S_{d,0}$	Displacement spectral value of the original structure
$S_{d,t}$	Target displacement spectral value of the damped structure
S_a	Spectrum acceleration
T	Fundamental period of an SDOF system
ζ	Damping ratio of an SDOF system
N_s	Total number of MYDs installed on the nth story
γ	Response mitigation ratio of the designed structure with MYDs
γ_d	Demanded response mitigation ratio
η	Structure seismic capacity redundancy
T_g	Characteristic period of the design response spectrum
θ_n	Interstory drift angle
$[\theta]$	Interstory drift angle limits
$[\theta]_{Li}$	Deformation limit corresponding to the ith performance level
$[\theta]_{Lu}$	Deformation limit corresponding to the ultimate performance level
Q_n	Story shear force

$$\zeta_{da} = \kappa\cdot\xi \tag{5}$$

The stiffness and damping parameters can be decoupled in form using Eq. (5). The stiffness and damping effects of an MYD can be directly reflected by parameters κ and ξ, respectively. Therefore, κ and ξ are considered as key design parameters for the design of a damped structure with MYDs. Note that stiffness parameter κ not only influences the additional damping ratio of the damped structure but also increases the stiffness of the structure and thereby affects its vibration period.

Plastic deformation may occur in the original structure in the event of severe earthquakes. In this case, the nonlinear plastic hysteretic damping ratio, ζ_{s0}, of the original structure can be obtained as follows:

$$\zeta_{s0} = \frac{W_{ps}}{4\pi W_{s0}} \tag{6}$$

where W_{ps} is the nonlinear plastic hysteresis energy of the original structure.

The nonlinear plastic hysteretic damping ratio, ζ_s, of the damped structure can be formulated as follows if dampers are installed in the structure:

$$\zeta_s = \frac{W_{ps}}{4\pi W_s} = \frac{W_{ps}}{4\pi W_{s0}}\cdot\frac{W_{s0}}{W_s} = \frac{W_{ps}}{4\pi W_{s0}}\cdot\frac{W_s - \sum W_{sd,i}}{W_s} = \zeta_{s0}\cdot(1-\kappa) \tag{7}$$

Therefore, the total equivalent damping ratio of the system after installing MYDs can be formulated as follows:

$$\zeta_{eq} = \zeta_0 + \zeta_s + \zeta_{da} = \zeta_0 + (1-\kappa)\cdot\zeta_{s0} + \kappa\cdot\xi \tag{8}$$

where ζ_0 is the inherent damping ratio of the original structure.

In engineering practice, MYDs are always accompanied by series-connected braces (Fig. 1). Therefore, the stiffness of the braces should be considered in the analytical model. In fact, the analytical model for an MYD used in design should be a combination of the MYD and its adjacent braces. A bilinear elastoplastic model is generally employed to model the hysteretic property of an MYD [33].

According to the bilinear model, the effective stiffness and equivalent damping ratio of an MYD for one hysteretic cycle can be determined as follows using Eqs. (9) and (10), respectively:

$$k_d = k_{d0}(1 + \alpha\mu - \alpha)/\mu \text{ and} \tag{9}$$

$$\xi = \frac{W_{d,i}}{4\pi W_{sd,i}} = \frac{2(1-\alpha)(\mu-1)}{\pi\mu(1 + \alpha\mu - \alpha)} \tag{10}$$

where k_{d0} is the initial stiffness of the damper, α is the post-to-pre-yielding stiffness ratio of the damper, and μ is the ductility factor of the damper, which is defined as the ratio of the maximum deformation to yielding deformation ($\mu = u_d/u_{dy}$).

Eq. (10) shows that the damping ratio, ξ, of an MYD basically depends on its ductility factor, μ, because yielding stiffness ratio α is typically constant for a specified design. Thus, the proposed UDR concept is approximately equivalent to the uniform ductility factor (UDF) concept. Therefore, the UDF concept is employed to simplify the design. The suggestions for the determination of an appropriate value of the UDF in practical design can be found in the Appendix A.

2.3. Utilization of an equivalent SDOF system

The design procedure is simplified by employing an equivalent SDOF system for the seismic response estimation and damper parameter determination of a multi-degree-of-freedom (MDOF) structure. As a conventional and widely-used structural type, shear-type frame structures are mainly considered in this study.

An N-story shear-type structure can typically be simplified into an MDOF system (Fig. 2).

The parametric definitions of the simplified MDOF system are as follows: the stiffness of the nth story is denoted as k_n; the effective stiffness of the supplemental damper installed on the nth story is denoted as $k_{d,n}$; the displacement and the interstory displacement of the nth story of the structure are denoted as u_n and Δu_n, respectively; the story displacement is normalized as ϕ_n by dividing it by the top displacement, u_{top}; the interstory displacement is normalized as δ_n by dividing it by the maximum interstory displacement, $\Delta u_{n,\max}$. These can

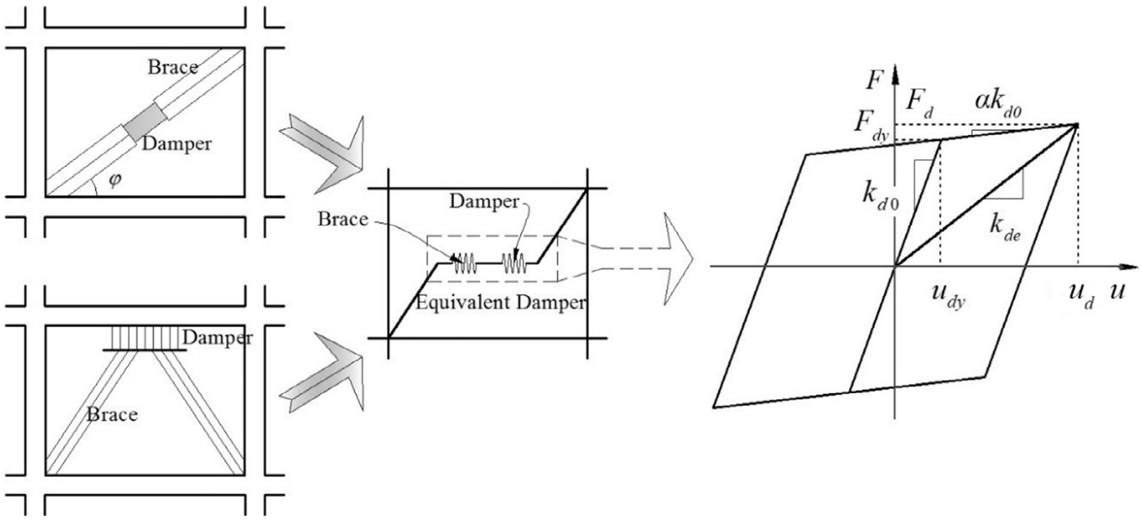

Fig. 1. Modeling of the damper–brace system.

be expressed as follows:

$$\phi_n = \frac{u_n}{u_{top}} \text{and} \tag{11}$$

$$\delta_n = \frac{\Delta u_n}{\Delta u_{n,\max}} = \frac{u_n - u_{n-1}}{\max\limits_{n=1}^{N}(u_n - u_{n-1})} = \frac{\phi_n - \phi_{n-1}}{\max\limits_{n=1}^{N}(\phi_n - \phi_{n-1})} \quad \cdots \quad (\phi_0 = 0) \tag{12}$$

The equivalent stiffness, $K_{eq,s}$, and equivalent mass, M_{eq}, of the corresponding SDOF system can be determined as follows if the deformed shape, ϕ_n, story stiffness, k_n, and story mass, m_n of the multistory shear-type structure are obtained [60]:

$$M_{eq} = \sum_{n=1}^{N} m_n \phi_n^2 \tag{13}$$

$$K_{eq,s} = \sum_{n=1}^{N} k_n (\phi_n - \phi_{n-1})^2 \tag{14}$$

The equivalent period, $T_{eq,s}$, is obtained as follows:

$$T_{eq,s} = 2\pi \sqrt{\frac{M_{eq}}{K_{eq,s}}} \tag{15}$$

The equivalent stiffness of the damped equivalent SDOF system after installing MYDs is expressed as follows:

$$K_{eq} = \sum_{n=1}^{N} (k_n + k_{d,n})(\phi_n - \phi_{n-1})^2 \tag{16}$$

Note that to simplify the derivation of equations, the normalized story displacement, ϕ_n, of the original structure and the damped structure with MYDs are assumed to be unchanged. The basis of this assumption is that the deformation shape of the structure does not significantly change as the rigidities of all stories should change coordinately according to the method proposed herein.

The generalized additional stiffness ratio, κ, can be rewritten as follows based on Eq. (3):

$$\kappa = \frac{\sum W_{sd,i}}{W_{s0} + \sum W_{sd,i}} = \frac{\sum_{n=1}^{N} k_{d,n} \delta_n^2}{\sum_{n=1}^{N} (k_n + k_{d,n}) \delta_n^2} \tag{17}$$

The relationship between K_{eq}, $K_{eq,s}$, and κ can be deduced as follows based on Eqs. (13), (16), and (17):

$$\frac{K_{eq,s}}{K_{eq}} = \frac{\sum_{n=1}^{N} k_n (\phi_n - \phi_{n-1})^2}{\sum_{n=1}^{N} (k_n + k_{d,n})(\phi_n - \phi_{n-1})^2} = \frac{\sum_{n=1}^{N} k_n \delta_n^2}{\sum_{n=1}^{N} (k_n + k_{d,n}) \delta_n^2}$$
$$= 1 - \frac{\sum_{n=1}^{N} k_{d,n} \delta_n^2}{\sum_{n=1}^{N} (k_n + k_{d,n}) \delta_n^2} = 1 - \kappa \tag{18}$$

Therefore, the equivalent period of the equivalent SDOF system

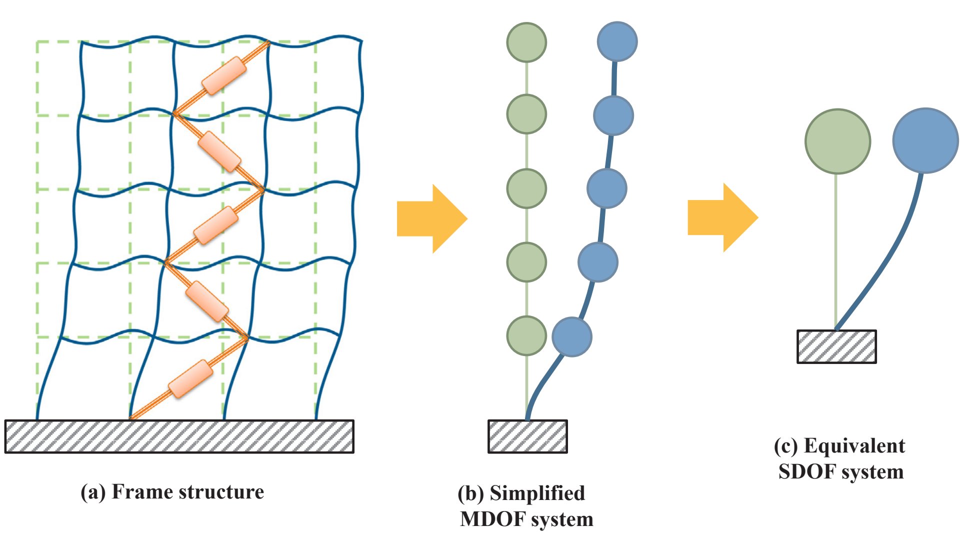

Fig. 2. Simplification of the shear-type frame structure.

with MYDs can be expressed as follows:

$$T_{eq} = T_{eq,s}\cdot\sqrt{1-\kappa} \tag{19}$$

For elastoplastic structures, the equivalent period, $T_{eq,s}$, can be obtained more conveniently through static pushover analysis or incremental dynamic analysis apart from using Eq. (15). The following procedure is suggested to obtain the equivalent period for a structure undergoing elastoplastic deformations: the relationship between top displacement u_{top} and base shear force V_{base} can be obtained using static pushover analysis or incremental dynamic analysis. Then, the u_{top} - V_{base} relationship is converted into an acceleration–displacement response spectra (ADRS) form as follows [33]:

$$S_d = u_{top}\cdot\frac{\sum_{n=1}^{N} m_n\phi_n^2}{\sum_{n=1}^{N} m_n\phi_n}S_a = \frac{V_{base}}{\sum_{n=1}^{N} m_n\phi_n^2} \tag{20}$$

where S_d and S_a are spectrum displacement and spectrum acceleration, respectively.

The approximate relationship between the S_d and S_a of an SDOF system is expressed as follows [60]:

$$S_d \approx \frac{T^2}{4\pi^2}(1-\zeta^2)S_a \approx \frac{T^2}{4\pi^2}S_a \tag{21}$$

where T and ζ are the fundamental period and damping ratio of the SDOF system, respectively.

The equivalent period can be calculated as follows based on Eqs. (20) and (21):

$$T_{eq,s} = 2\pi\sqrt{\frac{S_d}{S_a}} \tag{22}$$

2.4. Distribution of the key design parameters

A parameter distribution problem should be considered once the key design parameters (i.e., κ and ξ) are determined. This subsection mainly focuses on how to convert the global key design parameters (κ and ξ) into damper parameters for every story.

Stiffness parameter κ can be calculated as follows considering the MYDs, including braces, on the same story as one equivalent damper:

$$\kappa = \frac{\sum W_{sd,i}}{\sum W_{s0} + \sum W_{sd,i}} = \frac{\frac{1}{2}\sum_{n=1}^{N} k_{d,n}\delta_n^2}{\frac{1}{2}\sum_{n=1}^{N}(k_n + k_{d,n})\delta_n^2} = \frac{\{k_{d,n}\}^T\cdot\{\delta_n^2\}}{\{k_n\}^T\cdot\{\delta_n^2\} + \{k_{d,n}\}^T\cdot\{\delta_n^2\}},$$
$$= \frac{k_{d,\max}\{\widetilde{k}_{d,n}\}^T\cdot\{\delta_n^2\}}{k_{n,\max}\{\widetilde{k}_n\}^T\cdot\{\delta_n^2\} + k_{d,\max}\{\widetilde{k}_{d,n}\}^T\cdot\{\delta_n^2\}} \tag{23}$$

where $\{k_n\} = k_{n,\max}\{\widetilde{k}_n\}^T$ is the story effective stiffness vector of the original structure, $\{k_{d,n}\} = k_{d,\max}\{\widetilde{k}_{d,n}\}^T$ is the effective stiffness vector of the equivalent damper, including braces, $k_{n,\max}$ and $k_{d,\max}$ are the maximum values of the stiffness vectors of the original structure and damper, respectively, and $\{\widetilde{k}_n\}$ and $\{\widetilde{k}_{d,n}\}$ are the normalized stiffness vectors indicating the stiffness distribution patterns of the original structure and damper, respectively, along the height of the structure.

The stiffness distribution pattern, $\{\widetilde{k}_{d,n}\}$ of the damper along the height should be determined first to obtain the stiffness parameters, $\{k_{d,n}\}$, of the dampers on each story using Eq. (23). If no weak story exists in the main structure, the installed dampers and original structure are suggested to have the same stiffness distribution pattern for simplicity (i.e., $\{\widetilde{k}_{d,n}\} = \{\widetilde{k}_n\}$). Eq. (23) can now be simplified as follows:

$$\kappa = \frac{k_{d,\max}}{k_{n,\max} + k_{d,\max}} \tag{24}$$

Thus, the effective stiffness of the equivalent damper on each story can be obtained as follows:

$$\{k_{d,n}\} = k_{d,\max}\{\widetilde{k}_{d,n}\} = k_{n,\max}\frac{\kappa}{1-\kappa}\{\widetilde{k}_n\} = \frac{\kappa}{1-\kappa}\{k_n\} \tag{25}$$

The weak-story stiffness values in $\{k_n\}$ in Eq. (25) should be appropriately increased if weak stories exist in the original structure.

According to the UDF concept (i.e., $\mu_i = \mu$), the initial stiffness, $\{k_{d0,n}\}$, of the equivalent damper on each story can be obtained using Eqs. (9) and (25) if ductility factor μ is given.

The deformation, $u_{d,n}$, of the equivalent damper on each story is equal to the interstory deformation, Δu_n, of the structure. Hence, the yielding deformation of dampers can be expressed as follows:

$$\{u_{dy,\mathrm{n}}\} = \{u_{d,\mathrm{n}}\}/\mu = \{\Delta u_n\}/\mu \tag{26}$$

Eq. (26) shows that for a damped structure with MYDs, the UDF concept implies that the yielding deformation of the dampers on each story is approximately proportional to structure interstory deformation, and the proportional factor is the reciprocal of the UDF ($1/\mu$).

The yielding force of a damper can be calculated as $\{F_{dy,n}\} = \{k_{d0,n}\cdot u_{dy,n}\}$ after the equivalent parameters, $\{k_{d0,n}\}$ and $\{u_{dy,n}\}$, of each story are determined.

Considering actual constructional convenience, similar parameters should be merged to reduce the types of dampers. Dampers with relatively small calculated yielding forces can be removed.

Dampers are always installed at different locations on a certain story. Deformations at different locations are distinct because of the asymmetric planar distribution of stiffness and mass (i.e., torsion effect). With regard to a structure with a slight torsion effect, the distribution of the dampers on each story can be determined as follows: assuming that the total number of MYDs installed on the nth story is N_s, the parameters of the jth MYD can be calculated using $k_{d0,nj} = \frac{k_{d0,n}}{N_s}$ and $F_{dy,nj} = \frac{\Delta u_{n,j}}{\Delta \overline{u}_n}\cdot\frac{F_{dy,n}}{N_s}$, where $\Delta\overline{u}_n$ and $\Delta u_{n,j}$ are the average interstory displacement of the nth story and the interstory displacement at the location of the jth damper, respectively. For structures with severe torsion deformation, the torsional degree of freedom should be considered in the simplified MDOF model. This requires further study.

3. Demand-oriented design procedure

3.1. Response mitigation ratio

The aim of using dampers in structures is to mitigate dynamic response under external excitations and meet performance demand. Therefore, the demanded response mitigation ratio is employed herein as the controlling index in the design procedure.

The demanded response mitigation ratio, γ_d, is defined as follows after obtaining the predefined performance level and the response of the original structure:

$$\gamma_d = \frac{\text{Performance Level}}{\text{Response of Original Structure}}\cdot\frac{1}{\eta} \tag{27}$$

where η is the seismic capacity redundancy of the structure [33,61], and it can be used to flexibly control the performance design of damped structures.

A satisfactory design should meet the following requirement:

$$\gamma \leqslant \gamma_d \tag{28}$$

where γ is the response mitigation ratio of the designed structure with MYDs expressed as follows:

$$\gamma = \frac{\text{Response of Structure with Dampers}}{\text{Response of Original Structure}} \tag{29}$$

Using dampers is recommended when $\gamma_d \leqslant 90\%$ from an economical perspective.

In fact, design parameters can be obtained by solving Eq. (28) with "≤" replaced by "=".

$$\gamma = \gamma_d \tag{30}$$

Herein, Eq. (30) is referred to as the design equation. For an SDOF structure with an MYD, if structural response is estimated by the design

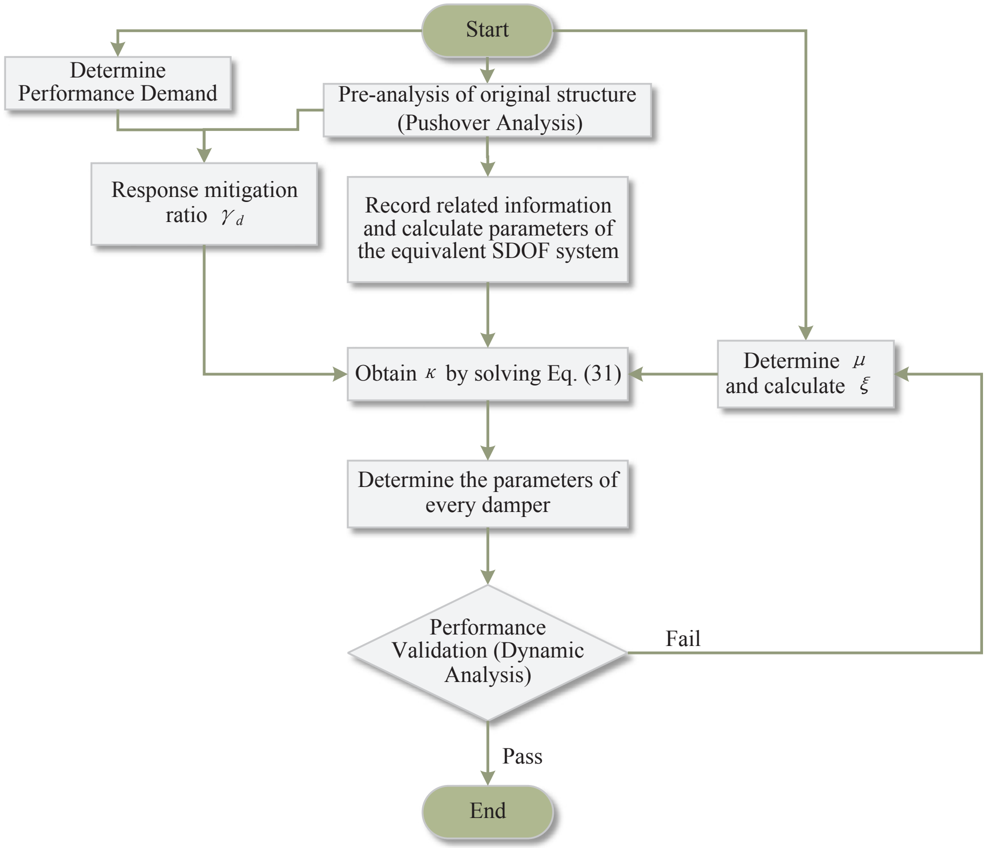

Fig. 3. Design flowchart of structure with MYDs based on UDR/UDF concept.

response spectrum, its design equation can be written as

$$\gamma = \frac{S_d(T_{eq},\ \zeta_{eq})}{S_{d,0}} = \frac{S_d(T_{eq,s}\cdot\sqrt{1-\kappa},\ \ \zeta_0 + (1-\kappa)\cdot\zeta_{s0} + \kappa\cdot\xi)}{S_{d,0}} = \gamma_d \tag{31}$$

where $S_{d,0}$ is the displacement response of the original structure, which can be obtained through static pushover analysis, and S_d is considered as a function with respect to the equivalent natural period and damping ratio.

3.2. Design procedure

With the abovementioned derivations and discussions, Fig. 3 shows the design flowchart of the elastoplastic structures with MYDs based on the proposed UDR design concept.

The following steps are involved in the design procedure for the damped structures with MYDs based on the UDF concept:

1. The design earthquake intensity and the corresponding threshold value of the performance index are determined according to the seismic design code or other special demands. Then, the structural model for seismic analysis is established, and the story mass, m_n, of the structure is recorded.
2. The static pushover analysis of the original structure is conducted, and the top displacement, u_{top}, and base shear force, V_{base}, curves are converted into the ADRS form using Eq. (20). The displacement spectral value, $S_{d,0}$, is determined based on the performance point obtained by the pushover analysis. Additionally, the corresponding value of the performance index can be acquired. Then, the response mitigation ratio, γ_d, is determined using Eq. (27). The target displacement spectral value of the damped structure is $S_{d,t} = \gamma_d\cdot S_{d,0}$. The following parameters are recorded: the story secant stiffness, k_n, corresponding to $S_{d,t}$ and the interstory displacement, Δu_n (k_n and Δu_n are required only for parametric distribution other than parametric design). The equivalent damping ratio, ζ_{s0}, and the equivalent period, $T_{eq,s}$, corresponding to the $S_{d,t}$ of the original structure are estimated based on a capacity curve.
3. The value of the UDF (i.e., μ) of dampers is selected based on the suggestions provided in the Appendix A. The corresponding UDR (ξ) is calculated using Eq. (10). The other key design parameter, κ, can be determined by solving the design equation (i.e., Eq. (31)). In addition, if the value of κ obtained using Eq. (31) is extremely high (approximately larger than 0.75), the original structure is considerably weakly resistant to earthquakes, and structural members must be redesigned to be stronger.
4. The parameters of the dampers on each story are determined using the parametric distribution approaches proposed in Section 2.4 based on the two determined parameters, μ and κ. Considering the practical cases (e.g., standardization, manufacturing capacity, etc.), the final parameters employed in practical applications may require adjustment. The adjusted parameters of any MYD are suggested to meet the following conditions: the actual yielding force should not be smaller than the designed value, and the actual yielding deformation should not be larger than the designed value.
5. The dynamic time-history analyses of the damped structure (using a 3D finite element model) should be performed to validate seismic performance. If seismic response does not exceed the threshold value of the performance index, the designed parameters are acceptable and the design procedure can be terminated. Otherwise, the parameters of MYDs should be adjusted until seismic performance is satisfied.

4. Design example

The proposed design method is exemplified using a nine-story

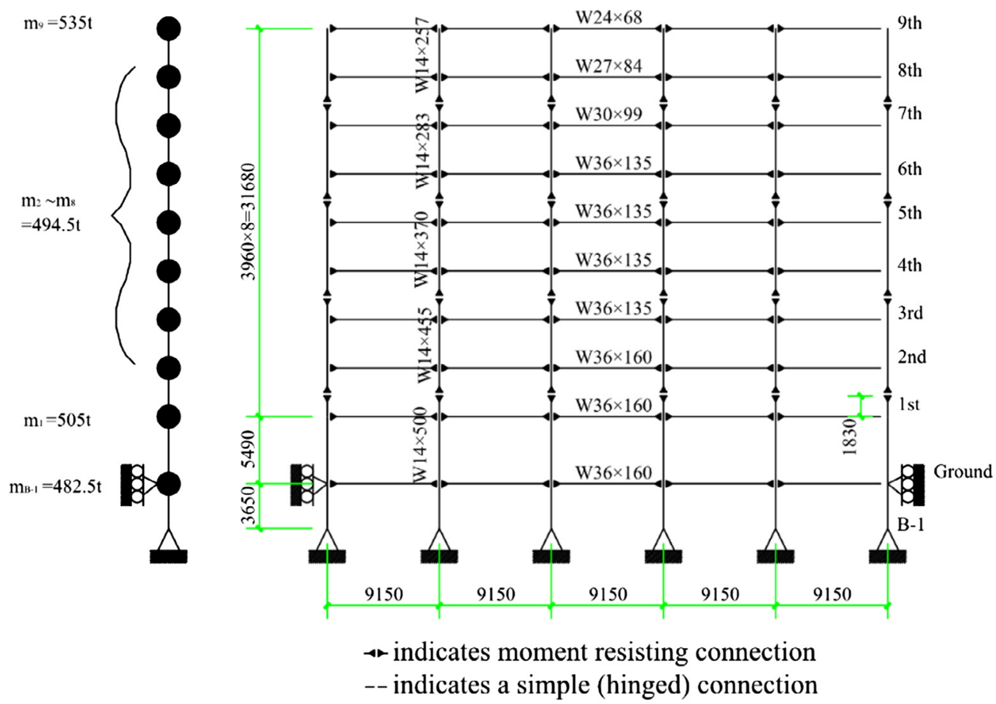

Fig. 4. Design example: nine-story steel frame structure [62]

structure model [62], as shown in Fig. 4.

The lateral load-resisting system of the structure comprises steel perimeter moment-resisting frames (MRFs). This study focuses on the in-plane (two-dimensional) analysis of the structure, and a single MRF is employed to describe this method. The columns and beams of the MRF are in the form of wide flanges. The columns and beams are made of steel with yielding strengths of 345 MPa and 248 MPa, respectively. Fig. 4 shows the section dimensions of the columns and beams. The peak ground acceleration (PGA) for the design is set as 300 Gal according to the Chinese code for the seismic design of buildings (CCSDB) [12]. The characteristic period, T_g, of the design response spectrum is set as 0.4 s. Table 2 lists the interstory drift angle limits under the frequent, fortification, and rare seismic levels according to the CCSDB [12].

The original damping ratio, ζ_0, and seismic capacity redundancy, η, of the structure are $\zeta_0 = 0.4\%$ and $\eta = 1.38$. The ultimate ductility factor, μ_u, and post-to-yielding stiffness ratio, α, of the selected steel damper are $\mu_u = 30$ and $\alpha = 0.04$. Table 3 lists the detailed model information. Modal analysis is conducted on the original structure, and the first three modal periods are obtained and compared with those obtained by Ohtori et al. [62], as listed in Table 4. The comparison of the first three modal periods shows that the model used in this study is largely identical to that employed elsewhere [62].

According to the design procedure given in Section 3.2, the following are the detailed design steps of the structure with MYDs:

(1) The model of the structure for analysis is established using SAP2000 [63], and the mass of each story, m_n, is prerecorded. Then, the pushover analysis of the original structure is conducted. The curves of the interstory drift angle and story shear force, θ_n - Q_n, corresponding to the performance point are obtained, as shown in Fig. 5. The interstory drift angle of the 9th story is significantly larger than those of the other stories, indicating that this story is relatively weak. This is mainly because the sections of the beams and columns of the upper stories are smaller than those of the lower stories, causing insufficient stiffness in the upper stories. Thus, two dummy elastic braces are installed on the 9th story to stiffen it (Fig. 9) and obtain a rational design. The values of the stiffness of the dummy elastic braces are empirically determined to make the 9th story not too weak, and these values are incorporated in the equivalent stiffness of the MYDs on the 9th story.

Table 2
Interstory drift angle limits under different seismic levels.

Seismic levels	[θ]
Frequent earthquake	0.4%
Fortification earthquake	0.6%
Rare earthquake	2%

Table 3
Model information.

Story	Story height (m)	Mass of story m_n (t)
9	3.96	494.5
8	3.96	494.5
7	3.96	494.5
6	3.96	494.5
5	3.96	494.5
4	3.96	494.5
3	3.96	494.5
2	3.96	494.5
1	5.49	505
B-1	3.65	482.5

Table 4
Modal periods of the original structure.

Modals	1st modal	2nd modal	3rd modal
Periods (s)	2.25	0.88	0.51
Periods (s) [62]	2.27	0.85	0.49

Then, the pushover analysis of the strengthened structure is conducted. Fig. 6 shows the corresponding θ_n - Q_n curve. Table 5 lists the results. According to the discussion in Section 3.1, the required

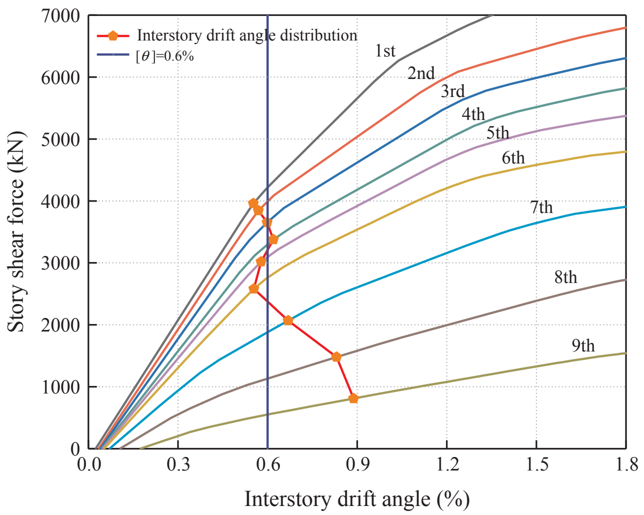

Fig. 5. θ_n - Q_n curves of the original structure.

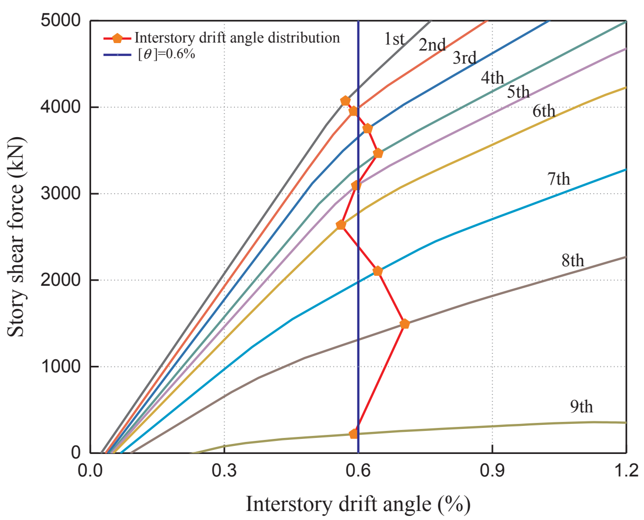

Fig. 6. θ_n - Q_n curves of the structure with dummy braces.

response mitigation ratio is $\gamma_d = \frac{0.6\%}{0.7\%}\cdot\frac{1}{1.38} = 62\%$ based on the structural response and seismic capacity redundancy of the structure.

(2) The top displacement and base shear force curves are converted into the ADRS form. The displacement spectral value corresponding to the performance point can be obtained (i.e., $S_{d,0} = 135$ mm). The desired displacement spectral value is $S_{d,t} = \gamma_d \cdot S_{d,0} = 84$ mm. Then, the analytical results of the target pushover step corresponding to $S_{d,t}$ are extracted. The equivalent story stiffness, k_n, can be approximately obtained by dividing the total shear force, Q_n, of the vertical structural members on each story by the interstory displacement, Δu_n, under the target analysis step. Table 6 presents the results of equivalent story stiffness. The equivalent damping ratio, ζ_{s0}, and equivalent period, $T_{eq,s}$, corresponding to the $S_{d,t}$ of the structure are estimated as $\zeta_{s0} = 6.2\%$ and $T_{eq,s} = 2.24$ s based on a capacity curve.

(3) According to the discussion in the Appendix A, the UDF is considered to be $\mu = 5.0 \leqslant \frac{0.6\%}{2.0\% \times 1.2}\mu_u = 7.5$ based on Eq. (A1). The corresponding UDR is found to be $\xi = 42.2\%$ using Eq. (10). Based on the designed response spectra function, $S_d(T_{eq}, \zeta_{eq})$, and demand displacement, $S_{d,t}$, it is found that $\kappa = 0.35$, $T_{eq} = 1.81$ s, and $\zeta_{eq} = 22.7\%$ by numerically solving Eq. (31).

(4) The parameters of the dampers on each story can be calculated using Eqs. (25) and (26). Table 7 lists the calculation results. Note that the designed parameters in Table 7 refer to the total value of all MYDs installed on one story. The parameters of each damper can be determined according to the discussion in Section 2.4 considering the actual locations of MYDs.

(5) According to the CCSDB [12], seven different earthquake waves are selected to conduct the dynamic time history analysis of the structure, including five natural seismic waves (NW1–NW5) and two artificial seismic waves (AW1 and AW2). Three seismic intensity levels are considered (i.e., frequent, fortification, and rare earthquake events mentioned in CCSDB) [12]. The natural earthquake waves (Table 8) are selected from the Pacific Earthquake Engineering Center ground motion database [64] considering the agreement between the response spectra of the waves and the design response spectrum and site condition. The artificial earthquake waves are generated using the trigonometric method [65] and then adjusted to match the design response spectrum [66–69]. Fig. 7 shows the corresponding response spectra, where the average response spectrum is approximately consistent with the design response spectrum.

Fig. 8 shows the interstory drift angle of the original structure under

Table 6
Pushover response of the structure corresponding to $S_{d,t}$.

Story	1	2	3	4	5	6	7	8	9
Shear force Q_n (kN)	1924	1868	1773	1637	1461	1246	994	705	381
Story displacement Δu_n (mm)	15	12	12	12	12	11	12	13	12
Story stiffness k_n (kN/mm)	128	156	148	136	122	113	83	54	32

Table 7
Designed parameters of MYDs.

Story number n	1	2	3	4	5	6	7	8	9
Effective stiffness of dampers $k_{d,n}$ (kN/mm)	69	84	80	74	66	61	45	29	17
Initial stiffness of dampers $k_{d0,n}$ (kN/mm)	299	362	344	318	283	264	193	126	74
Yielding deformation of dampers $\mu_{dy,n}$ (mm)	3.0	2.4	2.4	2.4	2.4	2.2	2.4	2.6	2.4
Yielding force of dampers $F_{dy,n}$ (kN)	896	869	825	762	680	580	463	328	177

Table 5
Pushover response of the structure at the performance point.

Story	1	2	3	4	5	6	7	8	9
Shear force Q_n (kN)	4072	3953	3752	3466	3093	2637	2104	1492	219
Interstory drift anlge (%)	0.57	0.59	0.62	0.64	0.60	0.56	0.64	0.70	0.59
Target interstory drift angle (%)	$[\theta] = 0.6$								
Required response mitigation ratioγ_d	62%								

Table 8
Detailed information of the natural seismic waves.

Name	RSN	Year	Magnitude	Event	Station
NW1	9	1942	6.5	Borrego	El Centro Array #9
NW2	15	1952	7.4	Kern County	Taft Lincoln School
NW3	40	1968	6.6	Borrego Mtn	San Onofre — So Cal Edison
NW4	55	1971	6.6	San Fernando	Buena Vista — Taft
NW5	86	1971	6.6	San Fernando	San Onofre — So Cal Edison

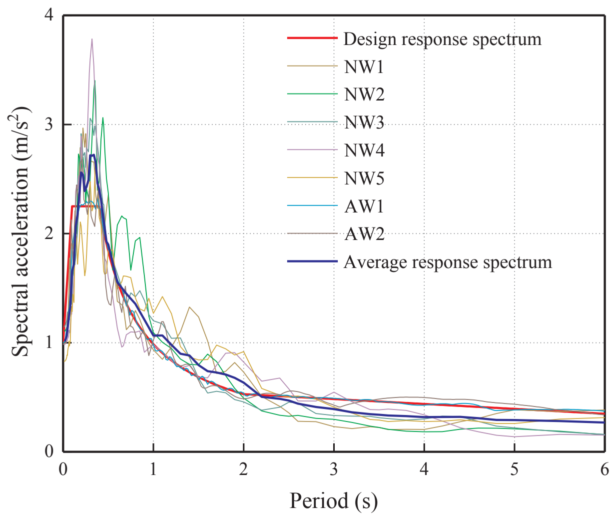

Fig. 7. Response spectra of the seismic waves.

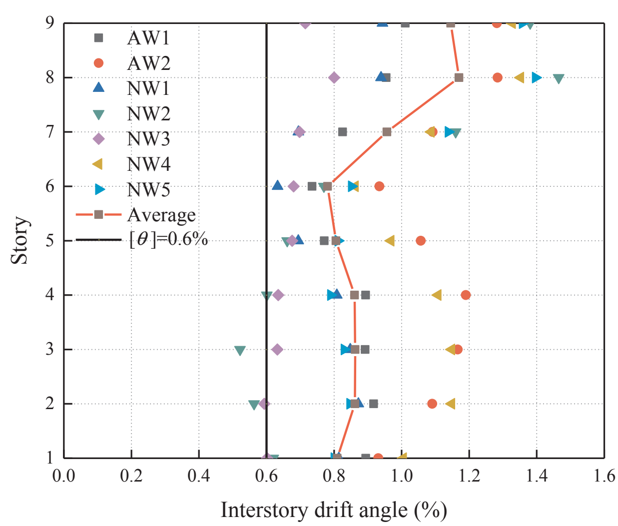

Fig. 8. Interstory drift angle of the original structure under the design earthquake (PGA = 300 Gal).

the design level earthquake (PGA = 300 Gal). The average interstory drift angle of the original structure does not satisfy the target interstory drift angle in terms of performance level.

(6) The parameters of MYDs are determined based on the design parameters listed in Table 7. Then, the designed dampers are added into the calculation model, and dynamic analyses are conducted using the seismic waves mentioned in the previous step. Fig. 9 shows the damped structure model.

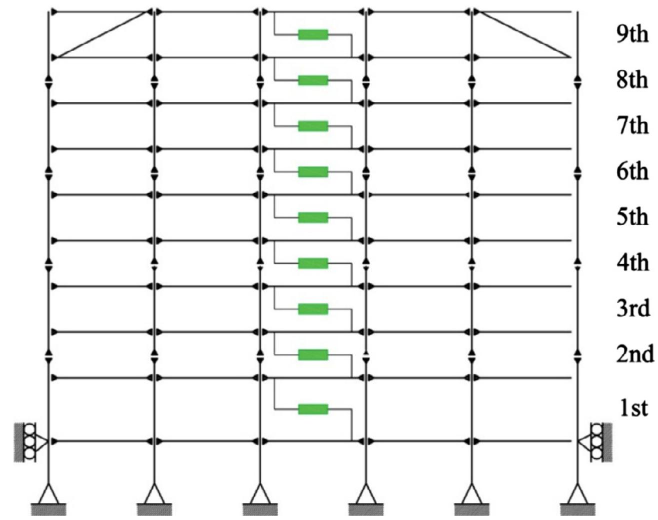

Fig. 9. Elevation of the MYD arrangement.

Fig. 10 shows the average interstory drift angle of the original structure and damped structure under frequent earthquakes (PGA = 110 Gal), fortification earthquakes (PGA = 300 Gal), and rare earthquakes (PGA = 510 Gal) according to the CCSDB [12].

The results show that the average response of the original structure without dampers does not meet the performance requirements under the frequent and fortification earthquakes. The interstory drift angles are effectively controlled after installing dampers. In brief, the seismic performance of the structure is significantly improved, and the average interstory drift angle is approximately equal to the interstory drift angle limit under the design earthquake, indicating that the proposed method is feasible.

Fig. 11 shows the hysteretic loops between the damping force and the deformation of the three MYDs installed at the 3rd, 6th, and 9th stories under seismic wave AW1 for PGA = 300 Gal. The results show that MYDs provide effective energy dissipation during the seismic event. Table 9 presents the ductility factors of the MYDs on each story under seismic wave AW1 for PGA = 110 Gal, 300 Gal, and 510 Gal. The results show that the ductility factors of the MYDs on each story are uniform under all earthquake events, thus conforming to the UDR concept. Notably, the UDR concept is a design assumption to simplify the calculation of the design parameters of dampers. In practical design, the requirement of the UDR concept does not need to be rigorously satisfied.

The structure is also designed using two other existing methods, that is, the EPRRC method proposed by Shen [54] and a trial method with identical MYDs, for the purpose of comparison and validation. The target responses of the maximum interstory drift angle of the three methods are set to be the same to make the results comparable. The design parameters of MYDs and the interstory drift angle responses are shown in Table 10 and Fig. 12, respectively.

Under the same maximum interstory drift angle, the total yielding forces of MYDs obtained using the UDR, EPRRC, and trial methods, which approximately imply the cost of MYDs, are calculated as $\sum_{\substack{n=1\\ \text{UDR}}}^{9} F_{dy,n} = 5580$ kN, $\sum_{\substack{n=1\\ \text{EPRRC}}}^{9} F_{dy,n} = 6006$ kN, and $\sum_{\substack{n=1\\ \text{Trial method}}}^{9} F_{dy,n} = 6372$ kN, respectively. The total yielding force of MYDs obtained using the UDR method proposed in this study is smaller than that obtained using the EPRRC (7.1% ↓) or trial methods (12.4% ↓), indicating that UDR method is more economical and rational. Note that the EPRRC and trial methods require numerous complex iterative analyses and repetitive pilot calculations to obtain rational parameters, while in the

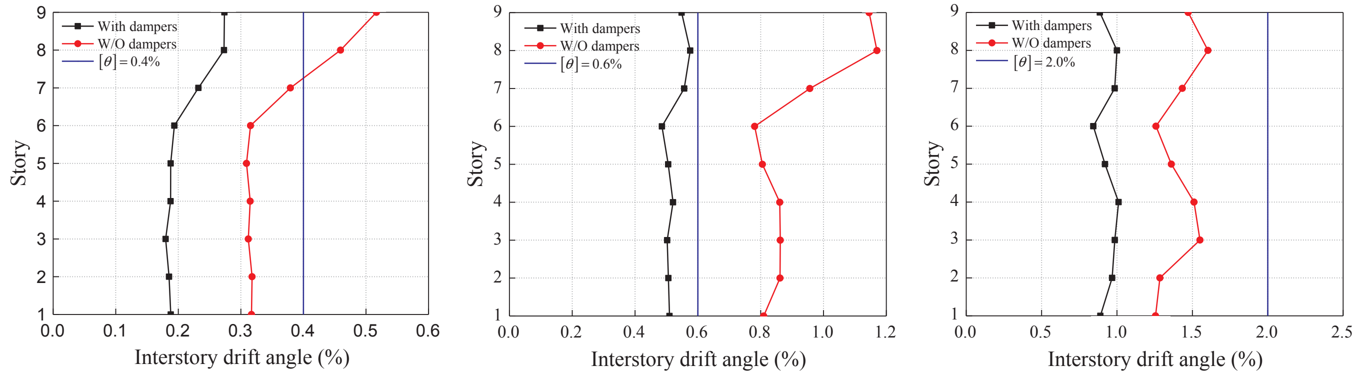

(a) Frequent earthquakes (b) Fortification earthquakes (c) Rare earthquakes

Fig. 10. Average interstory drift angle.

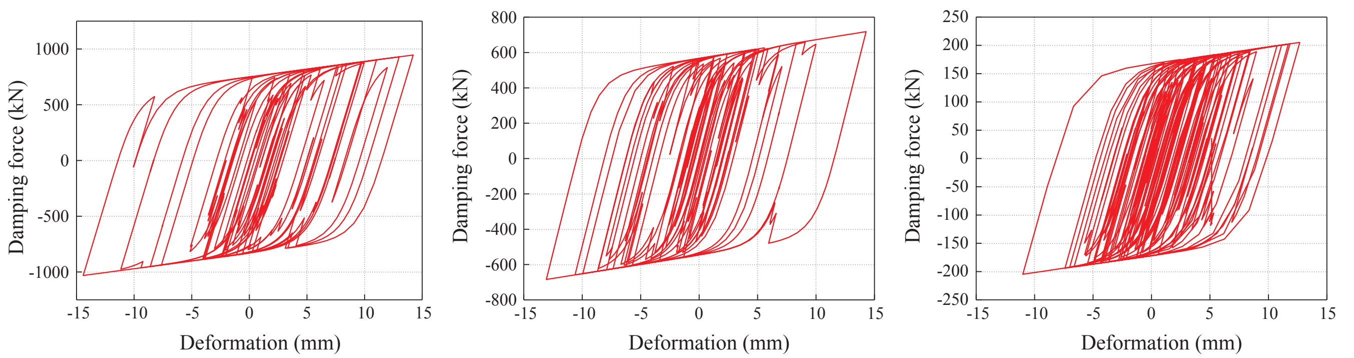

(a) 3rd story ($\mu = 5.93$) (b) 6th story ($\mu = 6.04$) (c) 9th story ($\mu = 5.49$)

Fig. 11. Hysteretic loops of MYDs.

Table 9
Practical ductility factors (μ) of MYDs.

Story	Ductility factors (μ)		
	PGA = 110 Gal	PGA = 300 Gal	PGA = 510 Gal
1st	2.25	6.39	12.52
2nd	2.39	6.38	11.86
3rd	1.68	5.93	10.87
4th	1.61	6.09	10.88
5th	1.76	5.78	11.27
6th	1.82	6.04	10.84
7th	2.07	6.13	10.01
8th	2.20	6.05	10.15
9th	1.79	5.49	8.52

UDR method, the design procedure and the distribution method of parameters are more succinct and easier. The comparison validates the rationality and demonstrates the implicit optimization effectiveness of the proposed design method.

5. Conclusion

A simplified design concept, termed the uniform damping ratio (UDR) concept, and a corresponding demand-oriented design method are proposed in this study for an elastoplastic structure with metallic yielding dampers (MYDs). A design philosophy is provided, including a method for obtaining the key design parameters and parametric distribution patterns of the structure. In addition, a detailed design procedure is presented, along with a design example. The following are the main conclusions of the study:

Table 10
Parameters designed using different methods.

Design method	Parameters	Story number n								
		1	2	3	4	5	6	7	8	9
UDR method	$k_{d0,n}$(kN/mm)	299	362	344	318	283	264	193	126	74
	$F_{dy,n}$(kN)	896	869	825	762	680	580	463	328	177
EPRRC method [53]	$k_{d0,n}$(kN/mm)	89	276	384	500	240	55	190	234	34
	$F_{dy,n}$(kN)	267	828	1152	1500	720	165	570	702	102
Trial method with identical MYDs	$k_{d0,n}$(kN/mm)	236	236	236	236	236	236	236	236	236
	$F_{dy,n}$(kN)	708	708	708	708	708	708	708	708	708

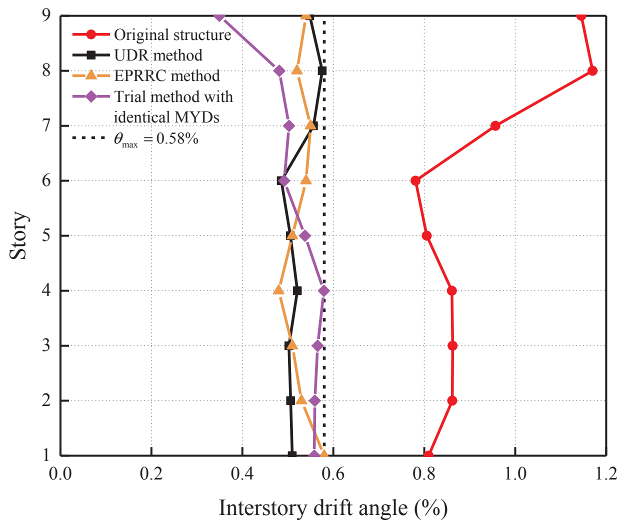

Fig. 12. Interstory drift angle responses of damped structure designed using different methods.

1. The UDR concept is a rational approach for obtaining a better design with the full use of the capacity of MYDs.
2. Based on the UDR concept, the stiffness and damping components in the damping ratio evaluation equation can be decoupled such that the two components can be separately designed, thereby simplifying the design of a damped structure with MYDs.
3. An equivalent SDOF system, pushover analysis, and a response mitigation ratio are introduced for the seismic performance evaluation in the parametric design for convenience (i.e., for reducing calculation effort).
4. For MYDs, the UDR concept is approximately equivalent to the UDF concept, which is convenient for applications.
5. A design example shows that the proposed design method is feasible, effective, purposive, and convenient.
6. The design philosophy of the UDR can be extended to designing structures with other types of dampers in future studies.

Acknowledgments

This study was supported by the Shanghai Pujiang Program (grant no. 17PJ1409200), the National Natural Science Foundation of China (grant no. 51778490), the Key Program for International S&T Cooperation Projects of China (grant no. 2016YFE0127600), the Fundamental Research Funds for the Central Universities (grant no. 22120180064), the Sichuan Department of Science and Technology (no. 2016JZ0009), the Natural Science Foundation of Shandong Province (grant no. ZR2018BEE033), and the Key Laboratory of Green Building in West China under (grant no. LSKF201804).

Appendix A. Additional suggestions for UDF determination

The target UDF, μ, of a damper must be determined based on damper performance. If the ultimate ductility factor of the damper is μ_u, the ductility factor, μ_{Lu}, of the damper under the highest fortification level earthquake should not exceed μ_u (i.e., $\mu_{Lu} \leqslant \mu_u/\gamma_d$) (e.g., Chinese Code for Seismic Design of Buildings (CCSDB) [12], setting $\gamma_d \geqslant 1.2$). The ductility factors under other seismic levels can be approximately determined based on the correlation (positive correlation) between the deformation of dampers and the structure, along with the relationship between different structural performance levels and their corresponding deformation limit values. If the deformation limit corresponding to the ith performance level is $[\theta]_{Li}$ and the deformation limit corresponding to the ultimate performance level is $[\theta]_{Lu}$, the ductility factor, μ_{Li}, of the damper corresponding to the ith performance level can be determined as follows:

$$\mu_{Li} \leqslant \frac{[\theta]_{Li}}{[\theta]_{Lu}}\mu_{Lu} \tag{A1}$$

References

[1] Soong TT, Spencer BF. Supplemental energy dissipation: state-of-the-art and state-of-the practice. Eng Struct 2002;24(3):243–59. https://doi.org/10.1016/S0141-0296(01)00092-X.
[2] Basu B, Bursi OS, Casciati F, Casciati S, Del Grosso AE, Domaneschi M, et al. A European association for the control of structures joint perspective. Recent studies in civil structural control across Europe. Struct Control Health Monit 2014;21(12):1414–36. https://doi.org/10.1002/stc.1652.
[3] Symans MD, Charney FA, Whittaker AS, Constantinou MC, Kircher CA, Johnson MW, et al. Energy dissipation systems for seismic applications: current practice and recent developments. J Struct Eng 2008;134(1):3–21. https://doi.org/10.1061/(ASCE)0733-9445(2008) 134:1(3).
[4] Pan C, Zhang RF, Luo H, Li C, Shen H. Demand-based optimal design of oscillator with parallel-layout viscous inerter damper. Struct Control Health Monit 2018;25(1). https://doi.org/10.1002/stc.2051.
[5] Pan C, Zhang RF. Design of structure with inerter system based on stochastic response mitigation ratio. Struct Control Health Monit 2018;25(6). https://doi.org/10.1002/stc.2169.
[6] Luo H, Zhang RF, Weng DG. Mitigation of liquid sloshing in storage tanks by using a hybrid control method. Soil Dyn Earthq Eng 2016;90:183–95. https://doi.org/10.1016/j.soildyn.2016.08.037.
[7] Chen QJ, Zhao ZP, Zhang RF, Pan C. Impact of soil-structure interaction on structures with inerter system. J Sound Vib 2018;433:1–15. https://doi.org/10.1016/j.jsv.2018.07.008.
[8] Zhang RF, Zhao ZP, Pan C. Influence of mechanical layout of inerter systems on seismic mitigation of storage tanks. Soil Dyn Earthq Eng 2018;114:639–49. https://doi.org/10.1016/j.soildyn.2018.07.036.
[9] Kim J, Shin H. Seismic loss assessment of a structure retrofitted with slit-friction hybrid dampers. Eng Struct 2017;130:336–50. https://doi.org/10.1016/j.engstruct.2016.10.052.
[10] Lee J, Kang H, Kim J. Seismic performance of steel plate slit-friction hybrid dampers. J Constr Steel Res 2017;136:128–39. https://doi.org/10.1016/j.jcsr.2017.05.005.
[11] Prestandard and commentary for the seismic rehabilitation of buildings (FEMA-356). Federal Emergency Management Agency; 2000.
[12] Chinese Code for Seismic Design of Buildings (GB50011-2010). Beijing, China: China Architecture & Building Press; 2010.
[13] Minimum design loads for buildings and other structures (ASCE7-10). American Society of Civil Engineers; 2010.
[14] Kelly JM, Skinner RI, Heine AJ. Mechanisms of energy absorption in special devices for use in earthquake resistant structures. Bull N Z Soc Earthquake Eng 1972;5(3):63–73.
[15] Foti D, Diaferio M, Nobile R. Dynamic behavior of new aluminum-steel energy dissipating devices. Struct Control Health Monit 2013;20(7):1106–19. https://doi.org/10.1002/stc.1557.
[16] Garivani S, Aghakouchak AA, Shahbeyk S. Numerical and experimental study of comb-teeth metallic yielding dampers. Int J Steel Struct 2016;16(1):177–96. https://doi.org/10.1007/s13296-016-3014-z.
[17] Lee CH, Lho SH, Kim DH, Oh J, Ju YK. Hourglass-shaped strip damper subjected to monotonic and cyclic loadings. Eng Struct 2016;119:122–34. https://doi.org/10.1016/j.engstruct.2016.04.019.
[18] Li HN, Li G. Experimental study of structure with "dual function" metallic dampers. Eng Struct 2007;29(8):1917–28. https://doi.org/10.1016/j.engstruct.2006.10.007.
[19] Sahoo DR, Singhal T, Taraithia SS, Saini A. Cyclic behavior of shear-and-flexural yielding metallic dampers. J Constr Steel Res 2015;114:247–57. https://doi.org/10.1016/j.jcsr.2015.08.006.
[20] Mahjoubi S, Maleki S. Seismic performance evaluation and design of steel structures equipped with dual-pipe dampers. J Constr Steel Res 2016;122:25–39. https://doi.org/10.1016/j.jcsr.2016.01.023.
[21] Basu D, Reddy PRM. A new metallic damper for seismic resilience: analytical feasibility study. Struct 2016;7:165–83. https://doi.org/10.1016/j.istruc.2016.06.011.
[22] Rai DC, Annam PK, Pradhan T. Seismic testing of steel braced frames with aluminum shear yielding dampers. Eng Struct 2013;46:737–47. https://doi.org/10.1016/j.engstruct.2012.08.027.

[23] Hsu HL, Halim H. Improving seismic performance of framed structures with steel curved dampers. Eng Struct 2017;130:99–111. https://doi.org/10.1016/j.engstruct.2016.09.063.
[24] Shen X, Wang XW, Ye Q, Ye AJ. Seismic performance of transverse steel damper seismic system for long span bridges. Eng Struct 2017;141:14–28. https://doi.org/10.1016/j.engstruct.2017.03.014.
[25] Han Q, Jia JF, Xu ZG, Bai YL, Song NH. Experimental evaluation of hysteretic behavior of rhombic steel plate dampers. Adv Mech Eng 2014;6. https://doi.org/10.1155/2014/185629.
[26] Hossain M, Ashraf M, Albermani F. Numerical modelling of yielding shear panel device for passive energy dissipation. Thin Wall Struct 2011;49(8):1032–44. https://doi.org/10.1016/j.tws.2011.03.003.
[27] Xu LY, Nie X, Fan JS. Cyclic behaviour of low-yield-point steel shear panel dampers. Eng Struct 2016;126:391–404. https://doi.org/10.1016/j.engstruct.2016.08.002.
[28] Saeedi F, Shabakhty N, Mousavi SR. Seismic assessment of steel frames with triangular-plate added damping and stiffness devices. J Constr Steel Res 2016;125:15–25. https://doi.org/10.1016/j.jcsr.2016.06.011.
[29] Cai KQ, Huang LZ. The design and application of the TADAS structure. Prog Steel Build Struct 2002;4(2).
[30] Bosco M, Marino EM. Design method and behavior factor for steel frames with buckling restrained braces. Earthq Eng Struct Dyn 2013;42(8):1243–63. https://doi.org/10.1002/eqe.2269.
[31] Qu Z, Kishiki S, Maida Y, Sakata H, Wada A. Seismic responses of reinforced concrete frames with buckling restrained braces in zigzag configuration. Eng Struct 2015;105:12–21. https://doi.org/10.1016/j.engstruct.2015.09.038.
[32] Wang CL, Chen Q, Zeng B, Meng SP. A novel brace with partial buckling restraint: an experimental and numerical investigation. Eng Struct 2017;150:190–202. https://doi.org/10.1016/j.engstruct.2017.06.031.
[33] Hao LF, Zhang RF, Jin K. Direct design method based on seismic capacity redundancy for structures with metal yielding dampers. Earthq Eng Struct Dyn 2017;47(2):515–34. https://doi.org/10.1002/eqe.2977.
[34] Skelton R, Maier H, Christ H. The Bauschinger effect, Masing model and the Ramberg-Osgood relation for cyclic deformation in metals. Mat Sci Eng A 1997;238(2):377–90. https://doi.org/10.1016/S0921-5093(97)00465-6.
[35] Ikhouane F, Manosa V, Rodellar J. Dynamic properties of the hysteretic Bouc-Wen model. Syst Control Lett 2007;56(3):197–205. https://doi.org/10.1016/j.sysconle.2006.09.001.
[36] Ismail M, Ikhouane F, Rodellar J. The hysteresis Bouc-Wen model, a survey. Arch Comput Method E 2009;16(2):161–88. https://doi.org/10.1007/s11831-009-9031-8.
[37] Guerrero H, Ji TJ, Teran-Gilmore A, Escobar JA. A method for preliminary seismic design and assessment of low-rise structures protected with buckling-restrained braces. Eng Struct 2016;123:141–54. https://doi.org/10.1016/j.engstruct.2016.05.015.
[38] Mazza F, Mazza M, Vulcano A. Displacement-based seismic design of hysteretic damped braces for retrofitting in-elevation irregular r.c. framed structures. Soil Dyn Earthq Eng 2015;69:115–24. https://doi.org/10.1016/j.soildyn.2014.10.029.
[39] Whittaker AS, Bertero VV, Thompson CL, Alonso LJ. Seismic testing of steel plate energy dissipation devices. Earthq Spectra 1991;7(4):563–604. https://doi.org/10.1193/1.1585644.
[40] Hossain MR, Ashraf M, Padgett JE. Risk-based seismic performance assessment of Yielding Shear Panel Device. Eng Struct 2013;56:1570–9. https://doi.org/10.1016/j.engstruct.2013.07.032.
[41] Moreschi LM, Singh MP. Design of yielding metallic and friction dampers for optimal seismic performance. Earthq Eng Struct Dyn 2003;32(8):1291–311. https://doi.org/10.1002/eqe.275.
[42] Yuri R, Jacob G. Optimal design of ADAS damped MDOF structures. Earthq Spectra 1999;15(2):317–30. https://doi.org/10.1193/1.1586043.
[43] Jensen HA, Sepulveda JG. On the reliability-based design of structures including passive energy dissipation systems. Struct Saf 2012;34(1):390–400. https://doi.org/10.1016/j.strusafe.2011.09.005.
[44] Liu W, Tong M, Lee GC. Optimization methodology for damper configuration based on building performance indices. J Struct Eng 2005;131(11). https://doi.org/10.1061/(ASCE)0733-9445(2005)131:11(1746).
[45] Occhiuzzi A. Additional viscous dampers for civil structures: analysis of design methods based on effective evaluation of modal damping ratios. Eng Struct 2009;31(5):1093–101. https://doi.org/10.1016/j.engstruct.2009.01.006.
[46] Manual JSSI. Design and construction manual for passively controlled buildings. Tokyo, Japan: Japan Society of Seismic Isolation; 2007.
[47] Lee J, Kim J. Development of box-shaped steel slit dampers for seismic retrofit of building. Eng Struct 2017;150:934–46. https://doi.org/10.1016/j.engstruct.2017.07.082.
[48] Benavent-Climent A, Mota-Páez S. Earthquake retrofitting of R/C frames with soft first story using hysteretic dampers: energy-based design method and evaluation. Eng Struct 2016;137:19–32. https://doi.org/10.1016/j.engstruct.2017.01.053.
[49] Bai JL, Ou JP. Earthquake-resistant design of buckling-restrained braced RC moment frames using performance-based plastic design method. Eng Struct 2016;107:66–79. https://doi.org/10.1016/j.engstruct.2015.10.048.
[50] Kim J, Seo Y. Seismic design of low-rise steel frames with buckling-restrained braces. Eng Struct 2004;26(5):543–51. https://doi.org/10.1016/j.engstruct.2003.11.005.
[51] Lin YY, Tsai MH, Hwang JS, Chang KC. Direct displacement-based design for building with passive energy dissipation systems. Eng Struct 2003;25(1):25–37. https://doi.org/10.1016/S0141-0296(02)00099-8.
[52] Guo YL, Zhang BH, Zhu BL, Zhou P, Zhang YH, Tong JZ. Theoretical and experimental studies of battened buckling-restrained braces. Eng Struct 2017;136:312–28. https://doi.org/10.1016/j.engstruct.2017.01.034.
[53] Chen ZY, Ge HB, Kasai A, Usami T. Simplified seismic design approach for steel portal frame piers with hysteretic dampers. Earthq Eng Struct Dyn 2007;36(4):541–62. https://doi.org/10.1002/eqe.643.
[54] Shen H, Zhang RF, Weng DG, Gao C, Luo H, Pan C. Simple design method of structure with metallic yielding dampers based on elastic–plastic response reduction curve. Eng Struct 2017;150:98–114. https://doi.org/10.1016/j.engstruct.2017.07.047.
[55] Benavent-Climent A. An energy-based method for seismic retrofit of existing frames using hysteretic dampers. Soil Dyn Earthq Eng 2011;31(10):1385–96. https://doi.org/10.1016/j.soildyn.2011.05.015.
[56] Choi H, Kim J. Energy-based seismic design of buckling-restrained braced frames using hysteretic energy spectrum. Eng Struct 2006;28(2):304–11. https://doi.org/10.1016/j.engstruct.2005.08.008.
[57] Habibi A, Chan RWK, Albermani F. Energy-based design method for seismic retrofitting with passive energy dissipation systems. Eng Struct 2013;46:77–86. https://doi.org/10.1016/j.engstruct.2012.07.011.
[58] Martínez CA, Curadelli O, Compagnoni ME. Optimal placement of nonlinear hysteretic dampers on planar structures under seismic excitation. Eng Struct 2014;65:89–98. https://doi.org/10.1016/j.engstruct.2014.01.030.
[59] Miguel LFF, Miguel LFF, Lopez RH. Robust design optimization of friction dampers for structural response control. Struct Control Health Monit 2014;21(9):1240–51. https://doi.org/10.1002/stc.1642.
[60] Chopra AK. Dynamics of structures: theory and applications to earthquake engineering. 4th ed. New Jersey, USA: Prentice Hall; 2001.
[61] Hao LF, Zhang RF. Structural safety redundancy-based design method for structure with viscous dampers. Struct Eng Mech 2016;59(5):821–40. https://doi.org/10.12989/sem.2016.59.5.821.
[62] Ohtori Y, Christenson RE, Spencer BF, Dyke SJ. Benchmark control problems for seismically excited nonlinear buildings. J Eng Mech 2004;130(4):366–85. https://doi.org/10.1061/(ASCE)0733-9399(2004)130:4(366).
[63] Wilson EL, Habibullah A. SAP2000: integrated finite element analysis and design of structures. Computers and Structures; 1997.
[64] Darragh B, Silva W, Gregor N. Strong motion record processing procedures for the PEER center. In: Proceedings of COSMOS workshop on strong-motion record processing, Richmond, California; 2004.
[65] Bozorgnia Y, Bertero V. Earthquake engineering: from engineering seismology to performance-based engineering. Boca Raton, Fla: CRC Press; 2004.
[66] Pan C, Zhang RF, Luo H, Shen H. Baseline correction of vibration acceleration signals with inconsistent initial velocity and displacement. Adv Mech Eng 2016;8(10). https://doi.org/10.1177/1687814016675534.
[67] Pan C, Zhang RF, Luo H, Shen H. Target-based algorithm for baseline correction of inconsistent vibration signals. J Vib Control 2018;24(12):2562–75. https://doi.org/10.1177/1077546316689014.
[68] Pan C, Zhang RF. EQSignal: a useful tool to process and generate earthquake signals; 2016. < http://www.eqsignal.com > .
[69] Atik LA, Abrahamson N. An improved method for nonstationary spectral matching. Earthq Spectra 2010;26(3):601–17. https://doi.org/10.1193/1.3459159.